J Mol Model (2009) 15:1213–1219
DOI 10.1007/s00894-009-0482-5

ORIGINAL PAPER

Contribution of arginine-glutamate salt bridges to helix stability

Kristin D. Walker · Timothy P. Causgrove

Received: 7 January 2009 / Accepted: 2 February 2009 / Published online: 5 March 2009

Abstract Peptide side chain interactions were studied by molecular dynamics simulation using explicit solvent on a peptide with the sequence AAARAAAAEAAEAAAARA. Three different protonation states of the glutamic acid side chains were simulated for four 20 ns runs each, a total simulation time of 240 ns. Two different salt bridge geometries were observed and the preferred geometry was found to depend on Glu — Arg residue spacing. Stable charge clusters were also observed, particularly in the fully charged peptide. Salt bridges were selectively interrupted upon protonation, with concomitant changes in secondary structure. The fully charged peptide was highly helical between residues 9 and 13, although protonation increased helicity near the N-terminus. The contribution of salt bridges to helix stability therefore depends on both position and relative position of charged residues within a sequence.

Keywords α−helix · Molecular dynamics · Peptide folding · Salt bridge interactions

Introduction

The in-depth study of model systems has been important in the development of biophysical theories and methods. Current knowledge of protein dynamics is based largely on the study of ligand binding of myoglobin, in which experiment and theory combined to give a comprehensive picture of the response of a globular protein to physical change [1, 2].

The most widely studied model system for protein folding has been the helix-coil transition in short alanine-based peptides. A driving force for analysis of the helix-coil transition was development of a theoretical framework for interpretation of both equilibrium [3, 4] and kinetic [5, 6] experiments. Early experimental studies were interpreted in terms of helix-coil theory; recently, comparisons between fast kinetic experiments and molecular dynamics simulations have shown success in modeling both the temperature dependence of the folding state and the timescale for folding [7, 8]. Such studies serve to both test the accuracy of force fields used in simulations [9] and to discern the relative importance of specific interactions for folding.

In order to model the fundamental forces that drive helix formation, many simulations have involved peptide sequences chosen for their simplicity, most often alanine-based sequences with specific substitutions. Charged residues such as lysine or arginine are often inserted into the sequence to induce helix formation [10] and confer high solubility for experimental studies. However, charged residues also add complexity to both experiment and modeling, as a charged residue can interact with solvent, with peptide backbone [11], or with other side chains. Stabilization of the α-helix by charged residues is well-known from experimental studies [12], and has therefore been a target of molecular dynamics simulations. Substitution of arginine residues into an alanine sequence (the Fs peptide) was shown to add stability due to the ability of arginine side chains to partially shield backbone hydrogen bonds from water [13].

Another factor in increasing complexity is side chain interactions such as salt bridges. One of the earliest known helix-forming peptides [14], the C-peptide of ribonuclease

K. D. Walker · T. P. Causgrove (✉)
Department of Physical & Environmental Sciences,
Texas A&M University-Corpus Christi,
6300 Ocean Drive, Unit 5802,
Corpus Christi, TX 78412-5802, USA
e-mail: tim.causgrove@tamucc.edu

A, contains glutamate at residue 2 and arginine at residue 10, which form a salt bridge in the crystal structure of the entire protein [15] and stabilize the isolated peptide [16]. An extensive series of experiments [11] by Baldwin's group showed that the salt bridge is a stabilizing element in the isolated C-peptide and can be distinguished from stabilization of the helix dipole by charged residues.

Subsequently, molecular dynamics simulations of the EK peptide [17], with three possible (i, i+3) glutamic acid-lysine salt bridges, showed that the primary helix stabilizing influence is sequestration of water from backbone hydrogen bonds by charged side chains, rather than salt bridge formation, an insight not available from experiment. In contrast, simulations [18] of peptides with three possible (i, i+4) Glu-Lys salt bridges (using Generalized Born solvation) had significant population of salt bridges. Recent simulations [19] have studied Glu-Arg salt bridge formation in a tetrapeptide. These simulations showed that the salt bridge is significantly populated and that its geometry is dependent upon the model used for solvent. Two differing geometries were identified, one in which the two Glu Oε atoms simultaneously interact with Arg Hε and an Arg Hη2 (a "paired" geometry). In the alternate geometry, a single Glu Oε atom simultaneously interacts with an Hη1 and an Hη2 of arginine (a "bifurcated" geometry). The population of the structures was dependent upon the water model used in the simulation. Simulations of the original C-peptide [20] showed a contribution from the Glu2-Arg10 salt bridge, but also included an aromatic-aromatic interaction between Phe8 and His12. Simulations of a peptide closely related to the C-peptide found that residues near Glu2 have a high probability of being part of helix nucleation [21]. However, the geometry of salt bridges and their role (if any) in stabilizing the α-helix structure was not reported.

Several questions remain about simulations involving side chain salt bridges, including whether arginine is inherently more likely to be involved in an intrahelix salt bridge than lysine, the effect of the spacing between residues, and whether the order of charges (i.e., whether the positive or negatively charged side chain is nearer the N-terminus) affects formation of a salt bridge. There are reasons to believe that the Glu-Arg (i, i+8) interaction is particularly effective in stabilizing the α-helix. First, the "paired" geometry found in Glu-Arg salt bridges is not likely to form with a Glu-Lys pair. Second, the large (i, i+8) spacing could allow a salt bridge to sequester solvent from two backbone hydrogen bonds, rather than one. And finally, side chain packing geometry and torsion energy may be different in the (i, i+8) arrangement than for closer spacings.

In order to study the population of (i, i+8) salt bridges and their effect on helix stability, a peptide with the sequence AAARAAAAEAAEAAAARA was simulated in explicit solvent. The peptide was designed to have two (i, i+8) interactions, R4-E12 and E9-R17. The peptide was simulated in three different protonation states. The unprotonated peptide was $E9^{-}E12^{-}$; a singly protonated peptide $E9^{0}E12^{-}$, and a doubly protonated form, $E9^{0}E12^{0}$. In all cases, arginine side chains were positively charged.

Methods

Each of the three protonation forms was simulated in four separate 20 ns runs. Simulations of each form of the peptide (unprotonated, E9 protonated and doubly protonated) were carried out at 300 K in the NPT ensemble with explicit solvent (TIP3P water). The NAMD software package [22] was used with the CHARMM27 force field for all simulations. Electrostatic potentials were calculated with the PME method, and non-bonded interactions were calculated using a switched potential with cutoffs of 10 Å and 12 Å. The SHAKE algorithm was used to constrain the length and angle of bonds involving hydrogen, allowing a time step of 2 fs. Non-bonded lists were updated every 10 steps with non-bonded interactions calculated every step. The Langevin piston method with an oscillation period of 100 fs and damping constant of 5 ps^{-1} was used to maintain a pressure of 1 bar. Electrostatic interactions were calculated every other step. Structures were saved every 5000 steps, such that a 20 ns run resulted in 2000 structures.

All of the 20 ns simulations were started from a nearly helical conformation. For each protonation form, the fully helical conformation was generated, then the system was solvated and chloride ions were added to maintain neutral charge. The system was minimized using the conjugate gradient method for 1000 steps with the backbone atoms fixed. The entire system was then minimized for 3000 steps, then heated to 300 K at constant volume with alpha carbons restrained. The volume of the system was equilibrated for 5000 steps with alpha carbons restrained and then equilibrated for 10000 steps with no restraints. The resulting structures for each of the three forms of the peptide, which were nearly helical, were used as the starting point for the four 20 ns runs of each form. The total simulation time was 240 ns.

The peptide was simulated in a rectangular box with side lengths of approximately 45 Å, 34 Å and 41 Å. The box contained 1804, 1803, and 1820 water molecules for the unprotonated, E9 protonated, and double protonated forms, respectively.

Analysis was carried out using the VMD software package [23]. RMSD of trajectories were measured relative to the initial (nearly helical) structure. Individual residues were deemed to be in a helix when φ=−67±30° and ψ=−47±30° *and* both adjacent residues met the same criteria. Therefore, the maximum number of helical residues for the 18-residue peptide was 16. Cluster analysis was performed using the

MMTSB Toolbox [24] with visualization of clusters in VMD.

Results

Salt bridge formation

In addition to R4-E12 and E9-R17 (i, i+8) interactions, simulations showed that stable (i, i+5) salt bridges R4-E9 and E12-R17 also form. Because different geometries may exist for a glutamate — arginine salt bridge, the interactions were measured by the distance between Glu Cδ and Arg Cζ to act as a centroid of the side chain distance. Figure 1 shows histograms of these distances for all four possible interactions. Salt bridges involving R17 are the most highly populated, reaching 73% occupancy for the E12-R17 salt bridge in the unprotonated form. The two (i, i+8) potential salt bridges are of opposite orientation; the more populated E12-R17 interaction opposes the helix dipole while the R4-E9 salt bridge is in the same direction as the helix dipole. For the (i, i+5) interaction, the more populated interaction also opposes the helix dipole. A possible reason for this correlation is that opposing interactions provides an opportunity for the salt bridge to be electrostatically stabilized by backbone hydrogen bonds.

It should be noted that a salt bridge between R17 and one Glu side chain does not necessarily preclude a second salt bridge involving R17 and the other Glu side chain; because Arg has two bonding sites (Hε paired with an Hη2 and an Hη1 paired with the other Hη2), a single Arg may be in a salt bridge with both Glu side chains. The R4-E12 interaction was

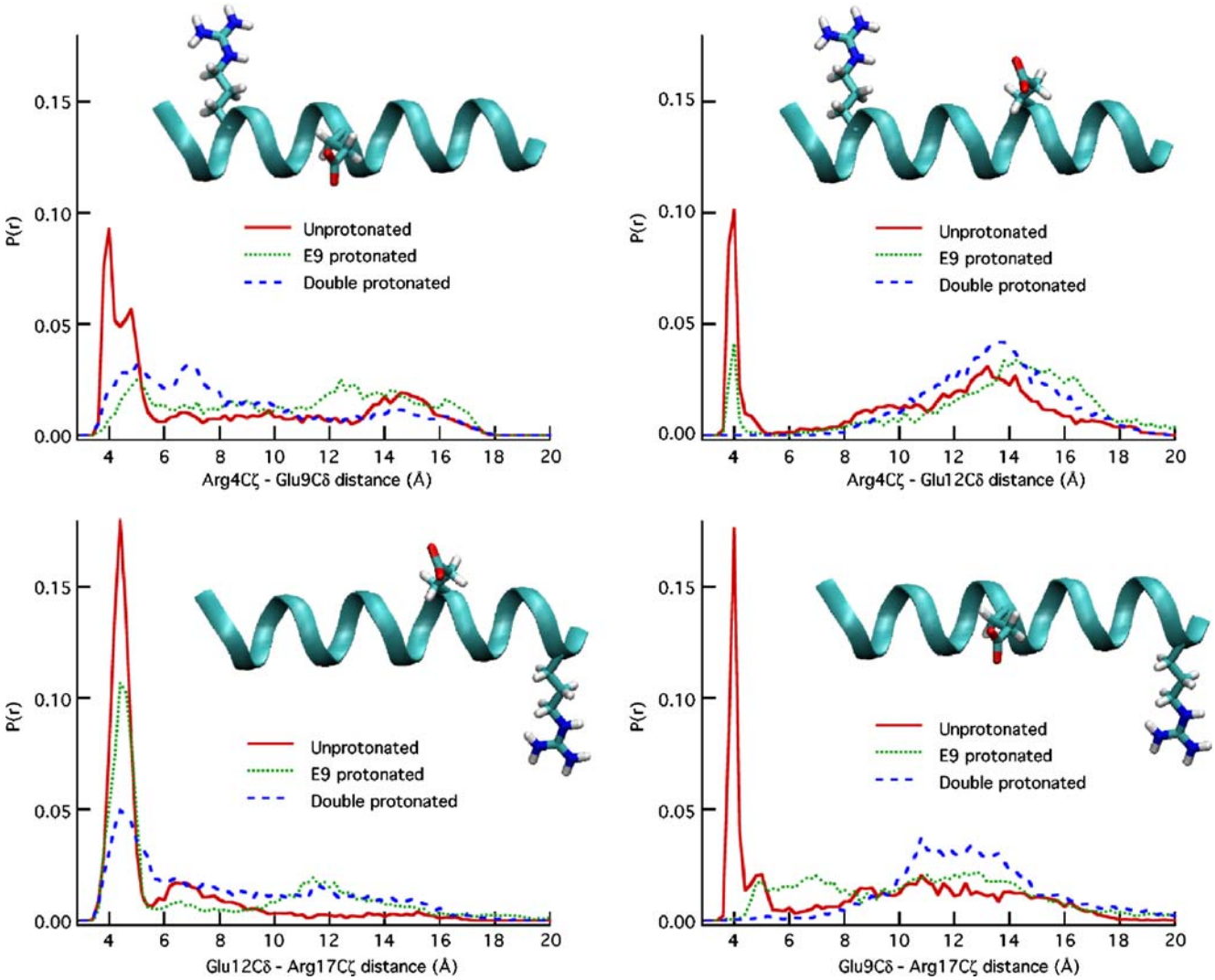

Fig. 1 Histograms of distance between arginine Cζ and glutamic acid Cδ for the four possible side chain interactions. The distances were binned in 0.2 Å increments with 8000 structures for each protonation state

least populated in the protonated form, although the population (24%) was still higher than the 10–20% reported for the (i, i+3) Glu — Lys interactions of the EK peptide [17].

Also of note in Fig. 1 is that there are two clear regimes of the Glu Cδ - Arg Cζ distance when in a salt bridge. This is most clearly seen in the histogram of distances for the R4-E9 interaction of the unprotonated peptide, which shows two resolved peaks of distances less than 6 Å. The first peak centered at 3.9 Å indicates a closer approach with less variation in distance, while the peak centered at 4.5 Å shows a greater variation in distance. Of the four possible glutamate — arginine interactions possible for this peptide, the (i, i+8) interactions (R4-E12 and E9-R17) almost exclusively correlate with the closer arrangement. For the (i, i+5) interaction, R4-E9 is capable of the close interaction, while E12-R17 is not.

Upon protonation of E9, the salt bridge it forms with R17 almost completely disappears, while the (i, i + 5) salt bridge loses the majority of its close association but is still capable of the slightly longer association. Although E12 is the same in protonated and unprotonated forms, the former shows a significant decrease in salt bridge population with both R4 and R17. This may be due to the contribution of charge clusters mentioned above, in which all four charged groups simultaneously interact. This was observed in only two of the four unprotonated simulations, but in cases when clusters formed, the arrangement was quite stable with residence times of more than 10 ns.

Protonating both E9 and E12 essentially eliminated the E9-R17 and R4-E12 interactions. The R4-E9 and E12-R17 interactions, which are notably both (i, i+5) interactions, were much less affected. In summary, (i, i+8) salt bridges in this peptide are close interactions which are interrupted by protonation and (i, i+5) salt bridges favor longer separations and are much less sensitive to protonation.

Solvation of backbone hydrogen bonds

In order to examine water sequestration from backbone hydrogen bonds, the number of waters in the first hydration shell, defined as an oxygen atom within 3.6 Å of a carbonyl oxygen in the backbone, is shown in Fig. 2 as a function of residue number for each of the protonation forms. In the unprotonated state, the carbonyl group of E12 is highly protected, and the carbonyl of R4 is somewhat protected. As expected, when the peptide is protonated, the salt bridges are much less populated and selected backbone carbonyls experience a higher level of solvation. It should be noted that although R17 is very often involved in salt bridges in the unprotonated state, the carbonyl groups of residues close to the C terminus are highly exposed to solvent. Therefore, an (i, i + 8) salt bridge does not protect two backbone carbonyl oxygen atoms from solvation.

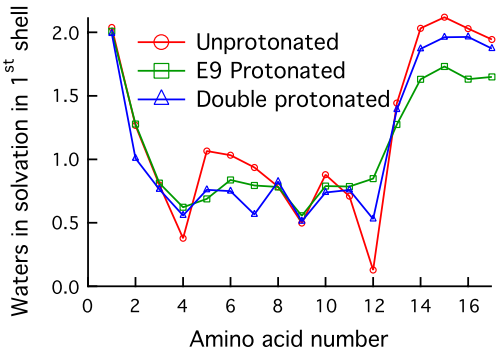

Fig. 2 Solvation of backbone carbonyl oxygen atoms for each protonation state. The first solvation shell was defined as the number of water molecules within 3.6 Å of the backbone carbonyl oxygen

Backbone RMSD

After starting the simulations in a (nearly) fully helical conformation, the root-mean square deviation (RMSD) of the backbone atoms as compared to their initial coordinates increased to a constant level with an exponential rate constant of about 1 ns (values ranging from 0.8 ns to 1.3 ns) for the unprotonated peptide. The RMSD at longer times had significant (up to 2.5 Å) fluctuations from their nominal level. The fluctuations in RMSD showed no obvious correlation with salt bridge formation. Each simulation was subjected to a cluster analysis over the last 10 ns of simulation based on pair-wise RMSD. Assignment to clusters depended primarily on the conformation of frayed terminal residues; formation of helix-turn-helix formation, as has been reported for the Fs peptide [25] was not observed.

Percent helix

As a result of the equilibration, production simulations were initially on average 76% helix, rather than 100% helix. The overall percent helix for each peptide showed considerable variation between different production runs of the same protonation state as well as the granularity expected for 16 possible helical residues. However, averaging the runs showed a consistent drop in helicity within the first few nanoseconds followed by a relatively stable period.

In order to ensure equilibration, the probability of each residue being in a helix was averaged over the last 2 ns of each simulation for each of the three protonation states. The results are shown in Fig. 3. Averaging over a longer time range (the last 10 ns of the simulations) produces similar graphs. For the unprotonated peptide, residues 9–13 are extremely likely to be helical, in keeping with the high occupancy of salt bridges. Surprisingly, the double protonated form was most helical overall, with a nearly constant fraction helix of 0.7 from residues 4 through 15. This form

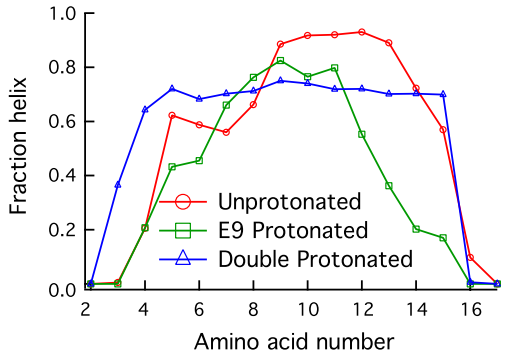

Fig. 3 Fraction of structures in a helix (helix probability) as a function of residue number. Residues 1 and 17 cannot be in a helix because they lack one of the neighboring residues

of the peptide was helical in spite of the relative absence of salt bridges. Furthermore, backbone solvation was not significantly lower than that of the much less helical E9 protonated form. Fitting the total percent helix as a function of time for each protonation form resulted in lifetimes of about 3 ns, significantly longer than changes in the RMSD. Although these lifetimes of ~3 ns are much faster than those observed experimentally [26], starting the simulation in a nearly helical form likely introduces a large driving force for unfolding and faster changes in the percent helix.

Discussion

Side chain geometry

Figure 1 shows two clear regimes of salt bridge formation, one favored by (i, i+8) side chain interactions in a narrow distance range around 3.9 Å and the other in a somewhat broader distance range centered near 4.5 Å. Examination of the simulations shows that the former is associated with a paired geometry between oxygens Oε1 and Oε2 of the Glu side chain and an Hη2 and Hε of Arg with two clear points of contact as shown in Fig. 4a. In contrast, the geometry favored by (i, i+5) interactions with a distance of about 4.5 Å is correlated with a bifurcated geometry in which a single Glu Oε interacts simultaneously with an Arg Hη2 and Hε. The other Arg binding site (Hη1 and the other Hη2) occasionally interacts with one of the glutamate oxygen atoms, but the site involving Hε is highly preferred. An example of the bifurcated geometry is shown in Fig. 4b.

The paired and bifurcated geometries of side chain salt bridges between Arg and Glu have been analyzed previously [27] using both explicit and generalized Born solvent. It was found that generalized Born solvation significantly over-stabilized salt bridges, whereas a hybrid solvent [19] was in good agreement with explicit solvent [27]. Generalized Born solvent favored a bifurcated geometry, while explicit and hybrid solvent favored a paired geometry. A bifurcated geometry as occurs predominantly with (i, i+5) interactions in this peptide has not previously been observed in explicit solvent.

As described in the results section above, an Arg side chain may be involved in more than one salt bridge at a time. The simulations showed formation of charge clusters in which involve three and at times all four charged side chains. One such charge cluster is shown in Fig. 4c. It is undetermined what the effect of including polarizability in the side chain model would be on the formation and stability of charge clusters.

These different geometries also help explain the dependence of the distance histograms in Fig. 1 on protonation state. The closer interactions largely disappear when the glutamate residue involved is protonated; a paired interaction is no longer possible. In contrast, protonation of a glutamate diminishes the occupation of the 4.5 Å salt bridge, but does not eliminate it. For example, in Fig. 1 the R4-E9 salt bridge is unaffected by protonation of E12, and the E12-R17 salt bridge is about half as common.

The preference of (i, i+8) interactions for a paired geometry and (i, i+5) interactions for a bifurcated (single-

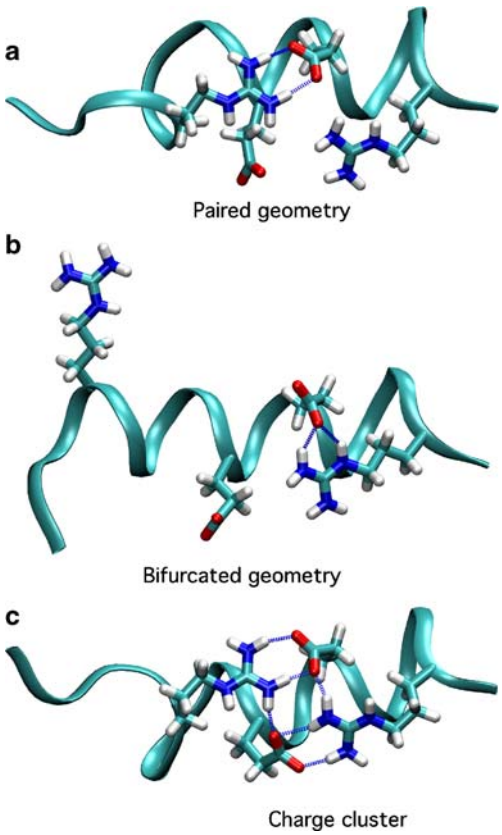

Fig. 4 Structures showing (**a**) a "paired" geometry, with Glu Cγ — Arg Cζ distance of about 3.9 Å, (**b**) a "bifurcated" geometry with Glu Cγ — Arg Cζ distance of 4.2 Å, and (**c**) a cluster interaction with all four charged side chains

oxygen) geometry may be due to side chain packing restraints, as the longer interaction must remain closer to the helix backbone, resulting in a "flat" interaction. However, the paired interaction may also be an artifact of the localized charges in the force field; this could be determined by using another model with more distributed charges.

Effect of protonation on helix formation

As shown in Fig. 3, the probability of a residue being in a helix varies significantly with protonation state. The unprotonated form has a highly helical core from residues 9 to 13. This is likely caused by the high occupation of R17 in salt bridges, both with E9 and E12. Because charge clusters sometimes form, the salt bridges often occur simultaneously; in fact, in all instances when the E9-R17 salt bridge was present, E12 was also involved. Figure 4 shows this salt bridge associated with a helical conformation, which is the predominant case. In this conformation, the backbone carbonyl groups of E9 and E12 are blocked from solvent access, but other backbone carbonyls are not. Residues near the N-terminus are predominantly random coil, but residues 5–9 are more than 50% helix. This generally corresponds with formation of salt bridges involving R4, whose carbonyl group is reasonably protected from solvation (Fig. 2).

In the E9 protonated form, residues 12 through 15 show a significant reduction in helicity. This appears to be a direct result of the loss of the E9-R17 salt bridge. A large increase in solvation of E12 also occurs, although solvation of E9 is not affected. Although the salt bridge E12-R17 is not interrupted, residues in this region of the peptide lose helicity, indicating that this interaction is not effective in stabilizing the helix.

The double protonated state of the peptide has the highest helicity overall, consistently about 70% helix from residues 4 through 15. In addition to affecting formation of salt bridges, charges on side chains are known to stabilize or destabilize the α-helix by interaction with the helix dipole [10]. The charge on the Arg side chains were not varied, but the positively charged R17 is helix stabilizing and R4 is destabilizing. Information on the extent of these effects along the helix is lacking, but it is interesting to note that Fig. 3 shows generally more helix near the C-terminus.

Because E9 is located near the center of the helix, its negative charge in the unprotonated form should have little effect on helix stability. Therefore, the large difference in fraction helix for residues 12 to 15 between the unprotonated and E9 protonated forms may be logically assigned to the absence of E9-R17 salt bridges.

The high percentage of helix observed in the double protonated form is somewhat more difficult to rationalize. The negatively charged side chain at position 12 should have a destabilizing effect, so protonating E12 should promote helix formation. However, the destabilizing effect is most likely to be felt between residue 12 and the N-terminus, while the simulations also show an increase in degree of helix near the C-terminus upon protonating E12, contrary to expectation.

Summary

Simulations of side chain interactions and their effect on helix formation in explicit solvent showed that Glu — Arg salt bridges are relatively highly populated in a short helical peptide. Spacings of (i, i+8) tend to favor a paired geometry, while Glu — Arg spacings of (i, i+5) more often favor a bifurcated geometry. The (i, i+8) spacing was found to protect only one backbone carbonyl group from solvation. Protonation of glutamate residues interrupted paired salt bridges, but not bifurcated salt bridges. The fraction of helical residues was found to change upon protonation, but salt bridge stabilization of the helix is difficult to separate from interactions of charged groups with the helix dipole. Therefore, the stabilization depends both on the position of the residue within a helix and the relative position of oppositely charged side chains. These results may be of use in designing coarse-grain models which attempt to include stabilization due to salt bridges.

Acknowledgments Simulations were performed on the High-Performance Computing Cluster at Texas A&M University-Corpus Christi, which is supported by grant #0321218 from the National Science Foundation. This work was supported by a grant from Texas Research Development Fund.

References

1. Frauenfelder H, McMahon BH (2000) Ann Phys 9:655–667
2. Fenimore PW, Frauenfelder H, McMahon BH, Parak FG (2002) Proc Natl Acad Sci USA 99:16047–16501
3. Zimm BH, Bragg JK (1959) J Chem Phys 31:526–535
4. Lifson S, Roig A (1961) J Chem Phys 34:1963–1974
5. Schwarz G (1968) Biopolymers 6:873–897
6. Poland D, Scheraga HA (1966) J Chem Phys 45:2071–2090
7. Snow CD, Nguyen H, Pande VS, Gruebele M (2002) Nature 420:102–106
8. Gnanakaran S, Garcia AE (2003) J Phys Chem B 107:12555–12557
9. Sorin EJ, Pande VS (2005) Biophys J 88:2472–2493
10. Shoemaker KR, Kim PS, York EJ, Stewart JM, Baldwin RL (1987) Nature 326:563–567
11. Fairman R, Shoemaker KR, York EJ, Stewart JM, Baldwin RL (1990) Biophys Chem 37:107–119
12. Pozo Ramajo A, Petty SA, Volk M (2006) Chem Phys 323:11–20
13. Garcia AE, Sanbonmatsu KY (2002) Proc Natl Acad Sci USA 99:2782–2787

14. Bierzynski A, Kim PS, Baldwin RL (1982) Proc Natl Acad Sci USA 79:2470–2474
15. Wlodawer A, Svensson LA, Sjölin L, Gilliland GL (1988) Biochemistry 27:2705–2717
16. Rico M, Gallego E, Santoro J, Bermejo FJ, Nieto JL, Herranz J (1984) Biochem Biophys Res Commun 123:757–763
17. Ghosh T, Garde S, Garcia AE (2003) Biophys J 85:3187–3193
18. Wang WZ, Lin T, Sun YC (2007) J Phys Chem B 111:3508–3514
19. Okur A, Wickstrom L, Layten M, Geney R, Song K, Hornak V, Simmerling C (2006) J Chem Theory Comput 2:420–433
20. Sugita Y, Okamoto Y (2005) Biophys J 88:3180–3190
21. Monticelli L, Tieleman DP, Colombo G (2005) J Phys Chem B 109:20064–20067
22. Kalé L, Skeel R, Bhandarkar M, Brunner R, Gursoy A, Krawetz N, Phillips J, Shinozaki A, Varadarajan K, Schulten K (1999) J Comput Phys 151:283–312
23. Humphrey W, Dalke A, Schulten K (1996) J Mol Graphics 14:33–38
24. Feig M, Karanicolas J, Charles L, Brooks I (2004) J Mol Graphics Modell 22:377–395
25. Zhang W, Lei H, Chowdhury S, Duan Y (2004) J Phys Chem B 108:7479–7489
26. Williams S, Causgrove TP, Gilmanshin R, Fang KS, Callender RH, Woodruff WH, Dyer RB (1996) Biochemistry 35:691–697
27. Okur A, Wickstrom L, Simmerling C (2008) J Chem Theory Comput 4:488–498